A Complete Surface Potential-Based Core Model for Undoped Symmetric Double-Gate MOSFETs*

He Jin[1,2,†], Zhang Lining[2], Zhang Jian[2], Fu Yue[2], Zheng Rui[2], and Zhang Xing[1,2]

(1 *Key Laboratory of Integrated Microsystems, Shenzhen Graduate School, Peking University, Shenzhen* 518055, *China*)
(2 *School of Electronic Engineering and Computer Science, Peking University, Beijing* 100871, *China*)

Abstract: A surface potential-based model for undoped symmetric double-gate MOSFETs is derived by solving Poisson's equation to obtain the relationship between the surface potential and voltage in the channel region in a self-consistent way. The drain current expression is then obtained from Pao-Sah's double integral. The model consists of one set of surface potential equations, and the analytic drain current can be evaluated from the surface potential at the source and drain ends. It is demonstrated that the model is valid for all operation regions of the double-gate MOSFETs and without any need for simplification (e.g., by using the charge sheet assumption) or auxiliary fitting functions. The model has been verified by extensive comparisons with 2D numerical simulation under different operation conditions with different geometries. The consistency between the model calculation and numerical simulation demonstrates the accuracy of the model.

Key words: bulk MOSFET limit; non-classical CMOS; double-gate MOSFET; device physics; surface potential-based model
PACC: 7340Q **EEACC**: 2560B; 2570D
CLC number: TN386.1 **Document code**: A **Article ID**: 0253-4177(2008)11-2092-06

1 Introduction

With the advance of double-gate (DG) MOSFET fabrication technologies[1~5], compact modeling for circuit simulation using DG MOSFETs has received a lot of attention[6~24]. Based on the intermediate variable used to calculate the output current, compact models can be categorized into three classes. The first approach uses the potentials at the two ends of the channel to calculate the terminal charges and currents. These models are called potential-based models and representative models have been developed by Taur, Adelmo, and Xin[10~18]. The second approach uses the density of the inversion charges at the two ends of the channel and formulates the model outputs in terms of these charge densities. Some models developed using this approach include the EKV-DG and previous BSIMDG[19~22]. The last approach uses the carrier concentration at the source and drain ends of the channel to calculate the drain current using a single function with the carrier concentration as the state variable[23,24]. Because the surface potential approach has been chosen as the industrial standard for the next generation bulk MOSFET model, it is desirable to use a similar approach to model the non-classical multiple-gate devices. Some surface potential based DG MOSFET models have been developed[25,26], but the derivations of these models are usually less rigorous than those for bulk MOSFETs.

In order to obtain a clearer understanding of the device physics of DG MOSFETs, similar to our previous work[27], a surface potential-based core model for the symmetric DG-MOSFET is proposed by rigorously solving Poisson's equation and Pao-Sah's double integral[28]. The model demonstrates that a surface potential versus voltage relationship and a drain current expression similar to those proposed by Brews for the single-gate (SG) bulk MOSFET[29] can be obtained for the symmetric DG MOSFETs. The accuracy of the model is verified by extensive comparisons with 2D numerical simulation under different operation conditions with different geometry. In the present form, the model does not include the influence of short-channel effects, quantum effects, or mobility degradation. These more advanced physical effects can be integrated into the presented model later using the modular approach.

2 Theoretical derivation of the DG-MOSFET model

Considering an ideal channel length, undoped n-

* Project supported by the National Natural Science Foundation of China (No. 90607017), the Competitive Earmarked Grant 611207 from the Research Grant Council of Hong Kong SAR, and the International Joint Research Program (NEDO Grant) from Japan (No. NEDO05/06. EG01)

† Corresponding author. Email: jinhe@ime.pku.edu.cn, frankhe@pku.edu.cn

Received 20 May 2008, revised manuscript received 29 June 2008

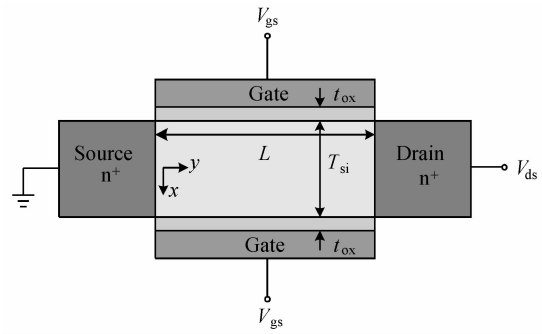

Fig. 1　Schematic diagram of the symmetric double gate MOSFET

channel symmetric DG-MOSFET, shown in Fig. 1, with only electrons as the conducting carrier, the Poisson's equation under the gradual-channel-approximation (GCA) takes the one-dimensional (1D) form:

$$\frac{\mathrm{d}^2\phi}{\mathrm{d}x^2} = \frac{qn_i}{\varepsilon_{si}}\mathrm{e}^{\frac{q(\phi-V)}{kT}} \tag{1}$$

where ϕ is the potential, V is the quasi-Fermi potential, and the other symbols have their common meanings. The assumption that conduction is dominated by electrons is valid when $\frac{q(\phi-V)}{kT} \geqslant 1$ where the hole density is negligible.

Due to the symmetry property of the DG MOSFETs, there is a point in the center of the silicon film where the vertical electric field is zero. Taking this point as the origin of the coordinate system, Equation (1) has to satisfy the following boundary conditions:

$$\frac{\mathrm{d}\phi}{\mathrm{d}x}(x=0)=0, \quad \phi\left(x=\pm\frac{T_{si}}{2}\right)=\phi_s \tag{2}$$

Equation (1) can be analytically solved giving the following[9~12]:

$$\frac{\mathrm{d}\phi}{\mathrm{d}x} = \sqrt{\frac{2n_ikT}{\varepsilon_{si}}}\sqrt{\mathrm{e}^{\frac{q(\phi-V)}{kT}}-\mathrm{e}^{\frac{q(\phi_0-V)}{kT}}} \tag{3}$$

where $\phi_0=\phi(x=0)$ is the centric potential.

From Eq. (3), we obtain the surface potential and surface field as follows:

$$\phi_s=\phi_0-2\frac{kT}{q}\ln\left[\cos\left(\sqrt{\frac{n_iq^2}{2kT\varepsilon_{si}}\mathrm{e}^{\frac{q(\phi_0-V)}{kT}}}\times\frac{T_{si}}{2}\right)\right] \tag{4a}$$

and

$$E_s=\left[\frac{2n_ikT}{\varepsilon_{si}}\mathrm{e}^{\frac{q(\phi_0-V)}{kT}}\right]^{1/2}\tan\left[\sqrt{\frac{n_iq^2}{2kT\varepsilon_{si}}\mathrm{e}^{\frac{q(\phi_0-V)}{kT}}}\times\frac{T_{si}}{2}\right] \tag{4b}$$

Following Boltzmann statistics, the surface potential and the inversion charge density can be expressed as

$$\phi_s=\phi_0-\frac{2kT}{q}\ln[\cos(m\sqrt{n_0})] \tag{5a}$$

$$Q_{in}=(2\varepsilon_{si}kT)^{1/2}\sqrt{n_0}\tan(m\sqrt{n_0}) \tag{5b}$$

where $n_0=n_i\mathrm{e}^{\frac{q(\phi_0-V)}{kT}}$ represents the electron concentration in the center of the silicon film and the factor $m=\frac{T_{si}}{2}\sqrt{\frac{q^2}{2\varepsilon_{si}kT}}$.

From Gauss's law, the following condition must be satisfied:

$$C_{ox}(V_{gs}-\Delta\varphi-\phi_s)=Q_{in}=\varepsilon_{si}\left.\frac{\mathrm{d}\phi}{\mathrm{d}x}\right|_{x=\pm\frac{T_{si}}{2}} \tag{6}$$

where C_{ox} is the gate oxide capacitance, and $\Delta\varphi$ is the work-function difference.

Substituting Eq. (3) into Eq. (6) leads to:

$$\frac{C_{ox}^2(V_{gs}-\Delta\varphi-\phi_s)^2}{2n_i\varepsilon_{si}kT}=\left[\mathrm{e}^{\frac{q(\phi_s-V)}{kT}}-\mathrm{e}^{\frac{q(\phi_0-V)}{kT}}\right] \tag{7}$$

From Eq. (7), we obtain the potential in the center of the silicon film:

$$\phi_0=V+\frac{kT}{q}\ln\left[\mathrm{e}^{\frac{q(\phi_s-V)}{kT}}-\frac{C_{ox}^2(V_{gs}-\Delta\varphi-\phi_s)^2}{2n_i\varepsilon_{si}kT}\right] \tag{8}$$

Substituting Eq. (8) into Eq. (5) results in a surface potential versus voltage expression:

$$\frac{C_{ox}(V_{gs}-\Delta\varphi-\phi_s)}{\sqrt{2n_i\varepsilon_{si}kT}}\mathrm{e}^{-\frac{q(\phi_s-V)}{2kT}}=\sin\left[\frac{T_{si}}{2}\sqrt{\frac{q^2n_i}{2\varepsilon_{si}kT}\left[\mathrm{e}^{\frac{q(\phi_s-V)}{kT}}-\frac{C_{ox}^2(V_{gs}-\Delta\varphi-\phi_s)^2}{2n_i\varepsilon_{si}kT}\right]}\right] \tag{9}$$

Equation (9) relates the surface potential to the gate voltage, quasi-Fermi potential, silicon film thickness, and the gate capacitance, which can be solved by numerical iteration such as Newton-Raphson (NR) to obtain the surface potential. Compared with previous works[9~24], this equation is derived more rigorously without any need for intermediate variables or auxiliary functions.

To apply Eq. (9) to obtain the drain current of DG MOSFETs, ϕ_s has to be evaluated at the source ($y=0$) and drain ($y=L$) ends with $V=0$ and $V=V_{ds}$. The results are denoted as $\phi_s=\phi_{SS}$ and $\phi_s=\phi_{SL}$, respectively. For a given V_{gs}, ϕ_s as a function of V can be solved using Eq. (9) along the channel from the source to the drain. The functional dependence between $V(y)$ and $\phi_s(y)$ is determined by the current continuity equation, which requires the DG-MOSFET drain current $I_{ds}=2\mu WQ\mathrm{d}V/\mathrm{d}y=\text{constant}$, independent of V or y. In the equation, the parameter μ is the effective mobility. As the given equation only accounts for half of the total channel current, the expression is multiplied by a factor of 2 to obtain the final current of the DG-MOSFET.

Following the Pao-Sah's double integral[27] and integrating $I_{ds}\mathrm{d}y$ from the source to the drain, the drain current can be written as

$$I_{ds}=2\frac{\mu W}{L}\int_0^{V_{ds}}Q(V)\mathrm{d}V \tag{10}$$

To continue the derivation, an equivalence of

Eq. (7) is obtained as expressed as

$$\frac{C_{ox}^2(V_{gs}-\Delta\varphi-\phi_s)^2}{2n_i\varepsilon_{si}kT}=e^{\frac{q(\phi_s-V)}{kT}}\left[1-e^{\frac{q(\phi_0-\phi_s)}{kT}}\right] \quad (11)$$

Solving the quasi-Fermi potential from Eq. (11) gives:

$$V=\phi_S+\frac{kT}{q}\ln\gamma^2+\frac{kT}{q}\ln\left[1-\exp\left(\frac{q(\phi_0-\phi_s)}{kT}\right)\right]-2\frac{kT}{q}\ln(V_{gs}-\Delta\varphi-\phi_S) \quad (12)$$

where γ is the body factor $\gamma=\frac{\sqrt{2n_i\varepsilon_{si}kT}}{C_{ox}}$.

Substituting $\phi_s-\phi_0$ from Eq. (5a) into Eq. (12), we obtain:

$$V=\phi_S+\frac{kT}{q}\ln\gamma^2+\frac{kT}{q}\ln\left[1-\cos^2(m\sqrt{n_0})\right]-2\frac{kT}{q}\ln(V_{gs}-\Delta\varphi-\phi_S) \quad (13)$$

Differentiating Eq. (13) yields:

$$dV=d\phi_S+\frac{kT}{q}\times\frac{m\,dn_0}{\sqrt{n_0}\tan(m\sqrt{n_0})}+2C_{ox}\frac{kT}{q}d\phi_s/Q_{in} \quad (14)$$

where

$$Q_{in}=C_{ox}(V_{gs}-\Delta\varphi-\phi_S) \quad (15)$$

Substituting Eqs. (5b) and (14) into Eq. (10) yields:

$$I_{ds}=2\frac{\mu W}{L}\int_0^{V_{ds}}Q_{in}dV=2\frac{\mu W}{L}\times\left[\int_{\phi_{SS}}^{\phi_{SL}}Q_{in}d\phi_S+\frac{mkT}{q}(2\varepsilon_{si}kT)^{1/2}\int_{n_{0S}}^{n_{0L}}dn_0+2C_{ox}\frac{kT}{q}\int_{\phi_{SS}}^{\phi_{SL}}d\phi_s\right] \quad (16)$$

Integrating Eq. (16), we obtain:

$$I_{ds}=2\frac{\mu W}{L}\left\{C_{ox}\left[(V_{GB}-\Delta\varphi)(\phi_{SL}-\phi_{ss})-\frac{1}{2}(\phi_{sL}^2-\phi_{ss}^2)\right]+2C_{ox}\frac{kT}{q}(\phi_{SL}-\phi_{ss})+\frac{T_{si}n_ikT}{2}\left[e^{\frac{q(\phi_{L0}-V_{ds})}{kT}}-e^{\frac{q\phi_{SO}}{kT}}\right]\right\} \quad (17)$$

where ϕ_{SS}, ϕ_{SL} are solutions to Eq. (9) corresponding to $V=0$ and $V=V_{ds}$, respectively.

Equation (17) is equivalent to the drain current expression in Refs. [11, 14, 23] if the appropriate transformation is performed. However, the derivation presented here is derived directly from the Poisson's equation and Pao-Sah's double integral, without the need for intermediate variables, auxiliary functions, or complicated spatial integration[11,14,23].

Combining Eqs. (7) and (17), the general drain current model is obtained as:

$$I_{ds}=\frac{2\mu WC_{ox}}{L}\left\{(V_{gs}-\Delta\varphi)\phi_s-\phi_s^2/2+\frac{2kT\phi_s}{q}+\left(\frac{kTn_iT_{si}}{2C_{ox}}\right)\times\left[e^{\frac{q(\phi_s-V)}{kT}}-\frac{C_{ox}^2(V_{gs}-\Delta\varphi-\phi_s)^2}{2n_i\varepsilon_{si}kT}\right]\right\}\Bigg|_{\phi_{SS},V=0}^{\phi_{SL},V=V_{ds}} \quad (18)$$

The DG-MOSFET drain current is expressed only in terms of the surface potentials at the source and drain ends.

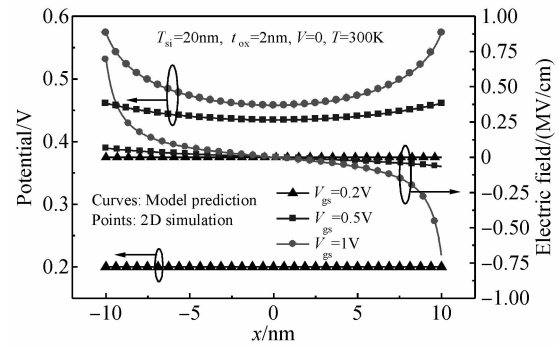

Fig. 2 Potential ϕ and electric field distribution across the silicon film for three different V_{gs}

3 Results and discussion

Based on the developed model, DG MOSFET characteristics from the linear to the saturation and from the sub-threshold to the strong inversion region can be calculated using Eq. (18) with the surface potential calculated using Eq. (9). The model calculation is compared with 2D numerical simulations by DESSIS-ISE®. A channel length (L) of 1μm, channel width (W) of 1μm, silicon oxide thickness (t_{ox}) of 2nm, a mid-gap gate structure, and a constant effective mobility of 400cm^2/(V·s) are assumed for both calculations.

Figure 2 shows the potential and electric field as functions of position in the silicon film for three different V_{gs}. Lines denote results calculated from the model and symbols represent results by 2D numerical simulation. Good agreements are observed. Under low V_{gs}, ϕ_s and ϕ_0 changes following V_{gs}, the electric field across the silicon film remains almost constant, and the "volume inversion effect" takes place. When V_{gs} increases, ϕ_s and ϕ_0 become decoupled and the surface electric field is much larger than the centric electric filed. The model predicts the potential across the whole silicon body successfully, thus capturing the important "volume inversion effect".

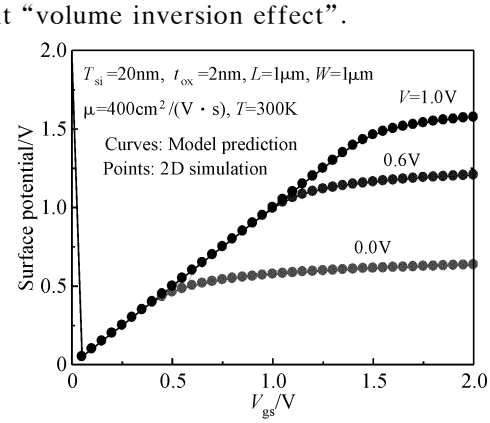

Fig. 3 Comparison of surface potential obtained from Eq. (9) (solid lines) with the 2D numerical results (points) for different quasi-Fermi potentials

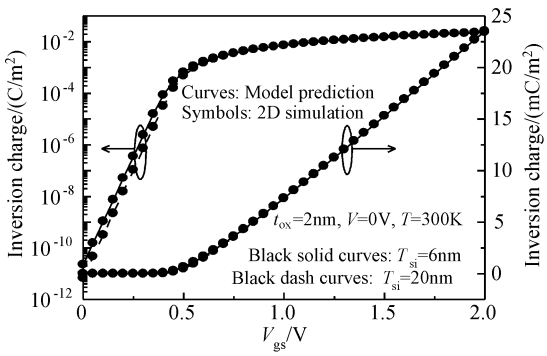

Fig. 4　Inversion charge characteristics obtained from Eq. (6) (solid and dash lines) based on calculated surface potential, compared with the 2D numerical simulation (points), both in logarithmic and linear coordinates

Figure 3 shows the surface potential versus gate voltage calculated from Eq. (9) and 2D numerical simulation for different quasi-Fermi-potential. The surface potential calculated by Eq. (9) is continuous and smooth in all operation regions from sub-thres-hold to strong inversion. The calculated results also agree well with the 2D numerical simulation. Figure 4 illustrates the comparison of the inversion charge density between the model prediction and the 2D numerical simulation for different silicon film thicknesses. Again, good agreement between the model calculation and 2D numerical simulation is obtained. The sub-threshold region charge increases as the silicon film thickness increases, while the strong inversion charge is independent of the silicon film thickness. This is again the unique "volume inversion effect" in undoped DG MOSFETs, which is correctly predicted by the model presented in this work.

From the device physics of DG MOSFETs, three distinct operational regions can be identified and predicted by Eq. (18). The characteristics of the different operational regions are discussed as follows:

(1) Linear region above the threshold: in this operational region the drain current is dominated by drift and the total drain current can be approximated by the first two terms of Eq. (18). Under this condition, the surface potential at the source can be approximated by a constant φ_m and the surface potential at the drain can be approximated by $\varphi_m + V_{ds}$, where

$$\varphi_m = \frac{kT}{q}\ln\frac{8\varepsilon_{si}kT}{qn_i^2T_{si}^2} \tag{19}$$

After the approximating the surface potentials, the drain current in the linear region above the threshold can be simplified to:

$$I_{ds} \approx \mu C_{ox}\frac{W}{L}[(V_{gs} - \Delta\varphi - \varphi_m)^2 - (V_{gs} - \Delta\varphi - \varphi_m - V_{ds})^2] = 2\mu C_{ox}\frac{W}{L}(V_{gs} - \Delta\varphi - \varphi_m - V_{ds}/2)V_{ds} \tag{20}$$

The drain current given in Eq. (20) is the drift component of the traditional surface-potential-based bulk MOSFET models that dominates in the strong inversion region.

(2) Subthreshold region: below threshold, the first two components in Eq. (18) are negligible. The fourth component (which is negative) cancels half of the third component in this operational region. As a result, the total drain current can be described by

$$I_{ds} \approx \frac{2\mu WC_{ox}}{L}\left[\frac{2kT}{q}(\phi_{SL} - \phi_{SS}) + \frac{kTn_iT_{si}}{2C_{ox}}\left(e^{\frac{q(\phi_{SL}-V_{ds})}{kT}} - e^{\frac{q(\phi_{SL}-V_{ds})}{kT}} + \frac{C_{ox}^2[(V_{gs} - \Delta\varphi - \phi_{ss})^2 - (V_{gs} - \Delta\varphi - \phi_{sL})^2]}{2n_i\varepsilon_{si}kT}\right)\right] \tag{21}$$

This drain expression can be further simplified to:

$$I_{ds} \approx \mu\frac{W}{L}kTT_{si}[n_{os} - n_{0d}] = \frac{\mu W}{L}kTn_iT_{si}e^{\frac{q(V_{gs}-\Delta\varphi-\varphi_m)}{kT}}(1 - e^{-qV_{ds}/kT}) \tag{22}$$

The sub-threshold current given in Eq. (22) is proportional to the silicon body thickness of the DG MOSFET and independent of t_{ox}. This is a typical characteristic resulting from the volume inversion effect that cannot be described by charge-sheet based models.

(3) Saturation region: this regime occurs when the contribution of the drain current at the drain end is small. Hence, the drain current is expressed as

$$I_{ds} = \frac{\mu W}{L}\left[2C_{ox}(V_{gs} - \Delta\varphi - \varphi_m)^2 + kTn_iT_{si}e^{\frac{q(V_{gs}-\Delta\varphi-\varphi_m)}{kT}}(1 - e^{-qV_{ds}/kT})\right] \tag{23}$$

The saturation current is mainly from the source inversion charge density as expected from the MOSFET device physics.

In order to verify the overall drain current model, a comparison between the model prediction and the 2D simulation is performed. Figure 5 shows the DG MOSFET I_{ds}-V_{gs} characteristics with different silicon film thicknesses, and Figure 6 shows the corresponding I_{ds}-V_{ds} curves under different gate voltages, calculated from the presented model and the 2D numerical simulation. Very good agreement is observed without using any fitting parameters in both figures. Especially, the volume inversion effect of DG-MOSFET demonstrated in Fig. 4 is described by the presented model as required by Eq. (22), matching the 2D numerical simulation very well.

Finally, we stress that the presented surface potential based model has three distinctive features: (1)

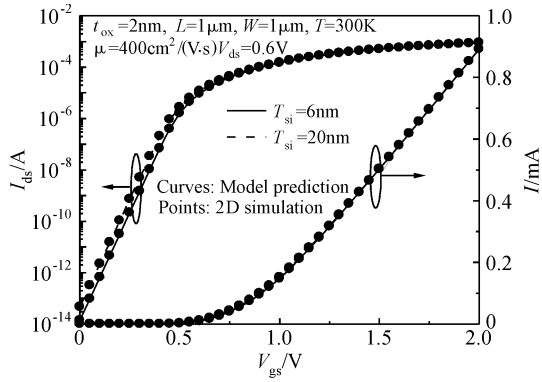

Fig. 5 I_{ds}-V_{gs} characteristics obtained from the surface potential-based model for two silicon film thicknesses (solid and dashed lines) compared with numerical simulations from DESSIS-ISE (points), both in logarithmic and linear coordinates

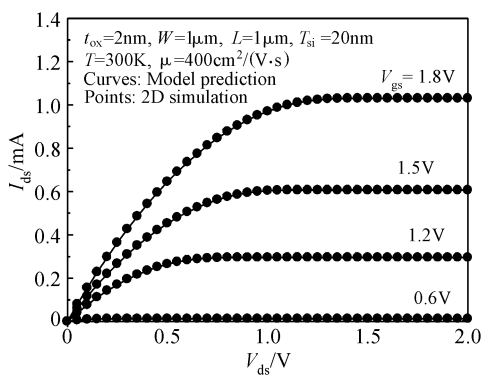

Fig. 6 I_{ds}-V_{ds} characteristics obtained from the surface potential-based model (solid lines) compared with numerical simulations from DESSIS-ISE (points)

A single set of the surface potential versus voltage equation is obtained from the exact Poisson equation solution in the undoped DG-MOSFET devices, analogous to that of the bulk MOSFETs, for which the complete surface potential equation is a base to develop a continuous model; (2) The drain current, obtained from Pao-Sah's dual integral, is described by one continuous function in terms of the surface potentials at the source and drain, tracing properly the transition between different DG-MOSFET operation regions without resorting to non-physical fitting-parameters; (3) The charge-sheet approximation, typically used in bulk MOSFET models to simplify Pao-Sah's dual integral for the drain current[27,28], is not invoked. Thus, the derived surface potential and drain current equations properly capture the DG-MOSFET's volume inversion effect.

4 Conclusion

A complete surface potential-based model for undoped symmetric DG-MOSFETs was presented. The presented model has three few unique features including: (1) A single set of the surface potential versus voltage equation is obtained from the exact solution of the Poisson's equation for undoped DG MOSFETs; (2) The drain current obtained from the Pao-Sah's double integral is described by one continuous function in terms of the surface potentials at the source and drain; and (3) No charge-sheet approximation is required to simplify Pao-Sah's double integral to obtain the drain current, which is reflected by the correct physical behaviors of the model under the volume inversion condition. Extensive verification with a 2D numerical simulator has been performed and the results indicated the presented model is very accurate and behaves well in all operation regions. In the present form, some advanced physical effects, such as short-channel effects, quantum effects, and high field transport have not been considered. They will be integrated into this model framework in the near future.

References

[1] ITRS. International technology roadmap for semiconductors, 2006. http://www.itrs.org

[2] Balestra F, Cristoloveanu S, Benachir M, et al. Double-gate silicon-on-insulator transistor with volume inversion: a new device with greatly enhanced performance. IEEE Electron Device Lett, 1987, 8: 410

[3] Tanaka T, Suzuki K, Horie H, et al. Ultrafast low-power operation of p-n double-gate SOI MOSFETs. Proc VLSI Technol Symp Tech Dig, 1994: 11

[4] Frank D J, Dennard R H, Nowak E, et al. Device scaling limits of Si MOSFETs and their application dependencies. Proceedings of the IEEE, 2001, 89: 259

[5] Colinge J P. Novel gate concepts for MOS device. 34th European Solid-State Device Research Conference ESSDERC, 2004: 45

[6] Shi X, Wong M. Analytical solutions to the one-dimensional oxide-silicon-oxide system. IEEE Trans Electron Devices, 2003, 50: 1793

[7] Pei G, Kan E C C. Independently driven DG MOSFETs for mixed-signal circuits: Part II applications on cross-coupled feedback and harmonics generation. IEEE Trans Electron Devices, 2004, 51 (12): 2094

[8] Mugnaini G, Iannaccone G. Physics-based compact model of nanoscale MOSFETs——part I: transition from drift-diffusion to ballistic transport. IEEE Trans Electron Devices, 2005, 52(8): 1795

[9] Taur Y. An analytical solution to a double-gate MOSFET with undoped body. IEEE Electron Device Lett, 2000, 21(5): 245

[10] Taur Y. Analytic solutions of charge and capacitance in symmetric and asymmetric double-gate MOSFET. IEEE Trans Electron Devices, 2001, 48(12): 2861

[11] Taur Y, Liang X, Wang W, et al. A continuous, analytical drain-current model for double-gate MOSFETs. IEEE Electron Device Lett, 2004, 25: 107

[12] Lu H, Taur Y. An analytic potential model for symmetric and asymmetric DG MOSFETs. IEEE Trans Electron Devices, 2006, 53(5): 1161

[13] Oritiz-Conde A, Garcia Sonchez F J, Malobabic S. Analytic solution of the channel potential in undoped symmetric dual-gate MOSFETs. IEEE Trans Electron Devices, 2005, 52(7): 1669

[14] Oritiz-Conde A, Garcia Sonchez F J, Muci J. Rigorous analytic solution for the drain current of undoped symmetric dual-gate MOS-

FETs. Solid State Electron,2005,49:640
[15] Ortiz-Conde A,García-Sánchez F J,Malobabic S,et al. Drain-current and transconductance model for the undoped body asymmetric double-gate MOSFET. Proc 8th Int Conf Solid-State and Integr Circuit Technol,Shanghai,China,2006:1239
[16] Ortiz-Conde A,García-Sanchéz F J,Muci J,et al. A general analytical solution to the one-dimensional undoped oxide-siliconoxide system. Proc IEEE Int Caribean Conf Circuits Devices and Syst,Playa del Carmen,Mexico,2006:177
[17] Ortiz-Conde A, García-Sánchez F J, Muci J, et al. A review of core compact models for undoped double-gate SOI MOSFETs. IEEE Trans Electron Devices,2007,54(1):131
[18] Ortize-Conde A,Garcia Sanchez F J. Unification of asymmetric DG,symmetric DG and bulk undoped-body MOSFET drain current. Solid-State Electron,2006,50:1796
[19] Shangguan W Z,Zhou X,Chandrasekaran K,et al. Surface-potential solution for generic undoped MOSFETs with two gates. IEEE Trans Electron Devices,2007,54(1):169
[20] He J,Xi J,Chan M,et al. A non-charge-sheet based analytical model of undoped symmetric double-gate MOSFETs using SPP approach. IEEE International Symposium on Quality of Electronic Design,2004:45
[21] Sallese J M,Krummenacher F,Prégaldiny F,et al. A design oriented charge-based current model for symmetric DG MOSFET and its correlation with the EKV formalism. Solid-State Electron,2005,49:485
[22] Roy A S,Sallese J M,Enz C C. A closed-form charge-based expression for drain-current in symmetric and asymmetric double gate MOSFET. Solid-State Electron,2006,50(4):687
[23] He J,Zhang J,Liu F,et al. A carrier-based approach for compact modeling of the long channel undoped symmetric double-gate MOSFETs. IEEE Trans Electron Devices,2007,54(5):1203
[24] He J,Bian W,Tao Y,et al. An explicit current-voltage model for undoped double-gate MOSFETs based on accurate yet analytic approximation to the carrier concentration. Solid-State Electron,2007,51(1):179
[25] CMC website of next generation MOSFET model standard phase-III evaluation results. http://www.eigroup.org/CMC
[26] Dunga M V,Lin C H,Xi X,et al. BSIM4 and BSIM multi-gate progress. Workshop on Compact Modelling,NSTI-Nanotech,Boston,USA,2006:658
[27] He J,Zhang L,Zhang J,et al. A complete surface potential-based core model for the undoped symmetric double-gate MOSFETs. IEEE Conference on Electron Devices and Solid-State Circuits,Tainan,2007:113
[28] Pao H C,Sah C T. Effects of diffusion current on characteristics of metal-oxide (insulator)-semiconductor transistors. Solid-State Electron,1966,9:927
[29] Brews J R. A charge sheet model of the MOSFET. Solid-State Electron,1978,21:345

非掺杂对称双栅的基于完整表面电势的核心模型*

何　进[1,2,†]　张立宁[2]　张　健[2]　傅　越[2]　郑　睿[2]　张　兴[1,2]

(1 北京大学深圳研究生院 集成微系统重点试验室，深圳　518055)
(2 北京大学信息科学技术学院，北京　100871)

摘要：通过求解 Poisson 方程自洽地得到了表面电势随沟道电压的变化关系,从而推出了非掺杂对称双栅 MOSFET 的一个基于表面势的模型.通过 Pao-Sah 积分得到了漏电流的表达式.该模型由一组表面势方程组成,解析形式的漏电流可以通过源端和漏端的电势得到.结果标明该模型在双栅 MOSFET 的所有工作区域都成立,而且不需要任何简化(如应用薄层电荷近似)和辅助拟合函数.对不同工作条件和不同尺寸器件的二维数值模拟与模型的比较进一步验证了提出模型的精度.

关键词：体 MOSFET 极限；非传统 CMOS；双栅 MOSFET；器件物理；表面势模型
PACC：7340Q　　**EEACC**：2560B；2570D
中图分类号：TN386.1　　**文献标识码**：A　　**文章编号**：0253-4177(2008)11-2092-06

* 国家自然科学基金(批准号:90607017),香港政府大学研究基金(批准号:611207)及日本国际联合研究项目(批准号:NEDOO5/06.EG01)资助项目
† 通信作者.Email:jinhe@ime.pku.edu.cn,frankhe@pku.edu.cn
2008-05-20 收到,2008-06-29 定稿